Supporting Information: Revisiting partition in hydrated bilayer systems

*João T. S. Coimbra, Pedro A. Fernandes, Maria J. Ramos**

UCIBIO, REQUIMTE, Departamento de Química e Bioquímica, Faculdade de Ciências, Universidade do Porto, Rua do Campo Alegre, s/n, 4169-007 Porto, Portugal

DETAILS

We provide the following data to support the main manuscript:

- Section 0: membrane's structural validation
- Section 1: supporting protocol
- Section 2: drugs' orientation and conformation
- Section 3: PMFs convergence.

Section 0: Membrane's structural validation.

In order to assess the quality of our membrane model system, we have performed a structural comparison of different quantities to experimentally determined ones. The following characteristics are evaluated: area per lipid (A_L), head-to-head bilayer thickness (D_{HH}), order parameters ($|S_{CD}|$), lipid diffusion coefficients (D_l), and density profiles. In all quantities, our system seems to be in line with experimental data. The results for these determinations are presented in Table S1 and Figure S1. Experimental data, when possible, is also presented.

Table S1. Structural results for the DMPC bilayer model considering the area per lipid (A_L), head-to-head bilayer thickness (D_{HH}), and lipid diffusion coefficients (D_l). Results are indicative of the last 20 ns portion of the 100 ns equilibration of the system. Experimental results are also depicted.

		A_L / nm^2		D_{HH} / nm		D_l / 10^{-8} cm^2·s^{-1}	
lipid	T / K	sim.	exptl.[1]	sim.	exptl.[2-3]	sim.	exptl.[4-6]
DMPC	310	0.604	-	3.64	-	6.80	
	303	-	0.599	-	3.44, 3.53		5.95, 9.00
	323	-	0.633	-	-		22.3

In Table S1, we see that both the area per lipid (A_L) and lipid diffusion coefficients (D_l) are within the established experimental range at 303 K and 323 K: A_L – 0.599 (303 K) < 0.604 (sim.) < 0.633 (323 K); and D_l – 5.95 (303 K) < 6.80 (sim.) < 22.3 (323 K). In addition, the bilayer thickness (D_{HH}) is also superior to the experimental data determined at 303 K: D_{HH} – 3.44/3.53 (303 K) < 3.64 (sim.).

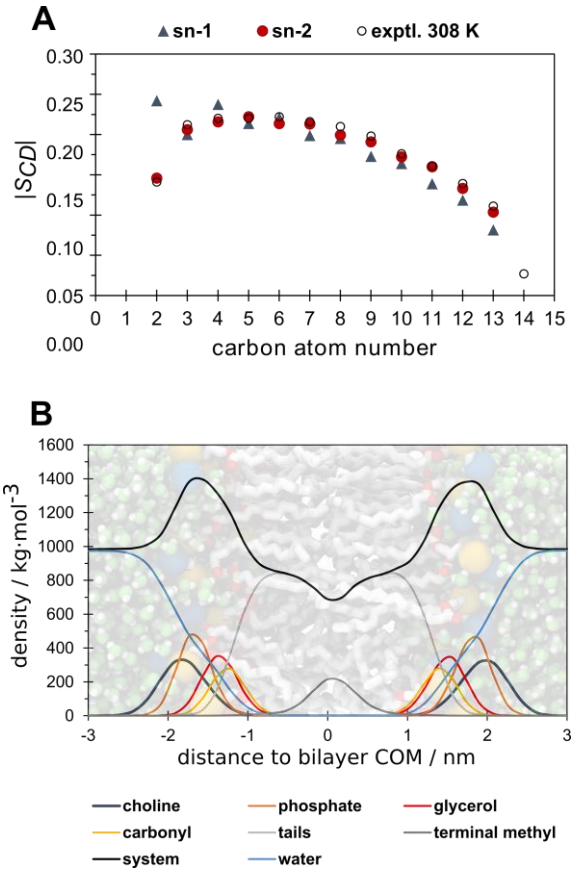

Figure S1. Order parameters ($|S_{CD}|$) (A) and density (B) profiles considering the last 20 ns of a total of 100 ns NPT equilibration simulation. Experimental data considering the order parameters was relative to the *sn-2* chain (the determination temperature is also presented).[7] Density profiles consider hydrogen atoms when present in the phospholipids' chemical groups. *The terminology used for the phospholipids' groups is derived from the parent molecules or functional groups that establish each phospholipid group. A membrane representation is added in the background of the density profiles.

Section 1: Supporting protocol

Molecular dynamics simulations. For the MD simulations additional technical aspects are presented here. Simulations were performed with the Verlet cutoff scheme that is compatible with the GPU acceleration code. We have used the LINCS constraint algorithm to all bonds,[8] which allowed for an integration time step of 2 fs. Considering the thermostat, the V-rescale thermostat was employed,[9] considering three coupling groups (water plus ions, bilayer, and drug-like compound). As for preserving a constant pressure for the system, the Parrinello-Rahman barostat [10-11] was active with a semi-isotropic scaling. Periodic boundary conditions (PBCs) were considered. Long-range electrostatic interactions were treated by a particle-mesh Ewald scheme.[12]

Constant-force pulling simulations. The pulling simulations were conducted, more or less with the same technical specifications as above, with an additional pull code. For generating the structures for the latter umbrella sampling simulations, a constant-force pulling was applied between the center-of-mass of two groups (in this case the bilayer and the drug-like compounds), using the "direction" pull coordinate geometry.

Umbrella sampling protocol. As for the umbrella simulations, an umbrella potential was applied to the same two groups as above, but instead with a cylinder reference geometry, with a radius of 1.5 nm. For the regions comprising the apolar region between [-0.2 – 0.3] nm, the umbrella force constant was increased from 1000 $kJ \cdot mol^{-1} \cdot nm^{-1}$ to 1500 $kJ \cdot mol^{-1} \cdot nm^{-1}$. This was conducted, as the superposition of the umbrella window's histograms was not achieved properly with the lower force constant. The PMFs were generated with the WHAM code.[13] The Bayesian bootstrap method was used to estimate the statistical error of the PMFs, using 200 bootstraps.[14]

Polarizability corrections. The polarization costs per compound are presented in Table S2.

Table S2. Polarization costs determined for each compound. For IBF, the polarization costs for the *cis* and *trans* carboxylic acid conformation are depicted.

compound	polarization costs / kcal·mol^{-1}
AML	-1.04
5PA	-0.66
DBS	-0.00
IBF (*cis*)	-0.06
IBF (*trans*)	-0.23

Flooding potential protocol. We have performed constant flooding simulations, for generating the structure for the constant pulling simulation from the bilayer center to the water slab. The flooding strength was set to 300 kJ·mol^{-1}. The same flooding strength was employed in the flooding simulations for each umbrella sampling window, with the exception of IBF. For IBF, a flooding strength of 200 kJ·mol^{-1} was employed in the water slab region (from 3.5 to 2.5 nm), whereas a 350 kJ·mol^{-1} flooding strength was applied for the rest of the umbrella sampling windows.

Dihedral PMFs. We have performed the umbrella sampling simulations for the dihedral angle conformational sampling with the AMBER 12 simulation package. The scanned coordinate is represented in Figure S6, representing the carboxylic acid dihedral. The umbrella sampling simulations were performed in explicit water systems, considering TIP3P water molecules. *NPT* production simulations of 200 ps were used to sample the PMFs from each umbrella sampling window. The reaction coordinate was defined as periodic (0º = 360º). A total of 121 windows were built using a consecutive umbrella sampling protocol (the final structure of the previous

window was used to generate the next window). Prior to the *NPT* production simulations of each window, a minimization stage of 2000 cycles was conducted using steepest descent (500 steps) and conjugated gradient minimization algorithms (1500 steps); and a *NVT* equilibration of 50 ps was also performed. Particle Mesh Ewald Molecular dynamics [12] were conducted with a cut-off of 0.8 nm. Langevin dynamics [15] was employed, maintaining a constant temperature of 300 K. A constant pressure of 1 bar was also set isotropically, using the weak-coupling barostat.[16] A harmonic force constant of 200 kcal·mol^{-1}·rad^{-2} was employed to maintain the dihedral angle at each umbrella sampling window sampled position. The PMFs were generated with the WHAM code.[13, 17]

Note: All system snapshots were processed with VMD.[18]

Section 2: drugs' orientation and conformation

Scheme S1. Reorientation of compounds within the bilayer and after the flooding simulation. Compound highlighted in red, represents the last structure of the 5 ns NPT equilibration; compound highlighted in blue stands for the last conformation of the flooding simulation (the orange arrow indicates the reorientation). The hydrated bilayer systems are superimposed in the scheme that is sectioned for highlighting the compounds within the bilayer. DBS compound is not shown, as no relevant orientation is pronounced by the chosen vector.

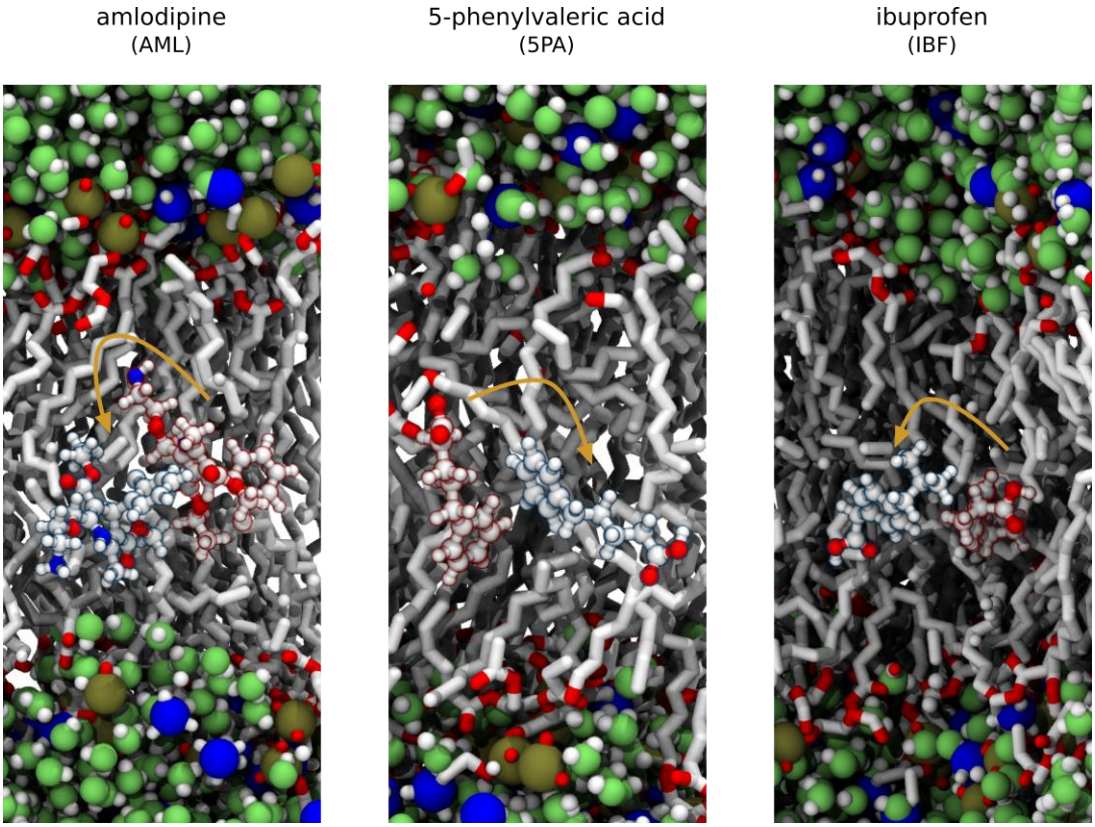

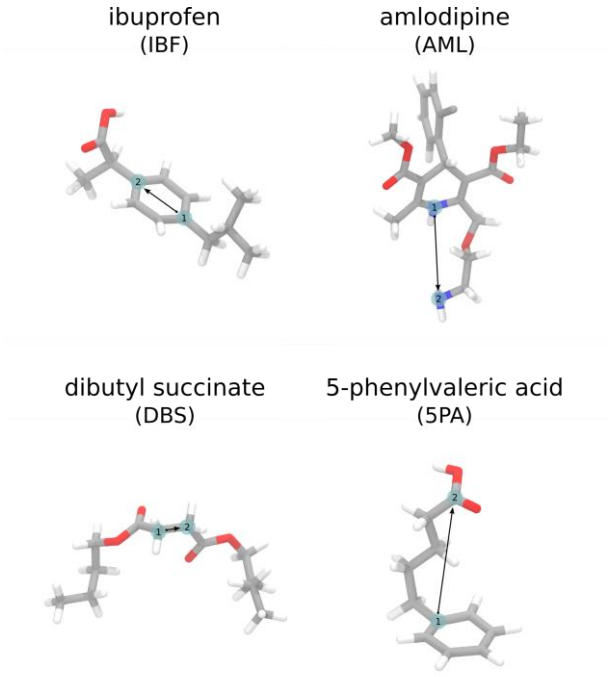

Figure S2. Drugs' vector employed for the orientation analysis relative to the bilayer normal (z axis).

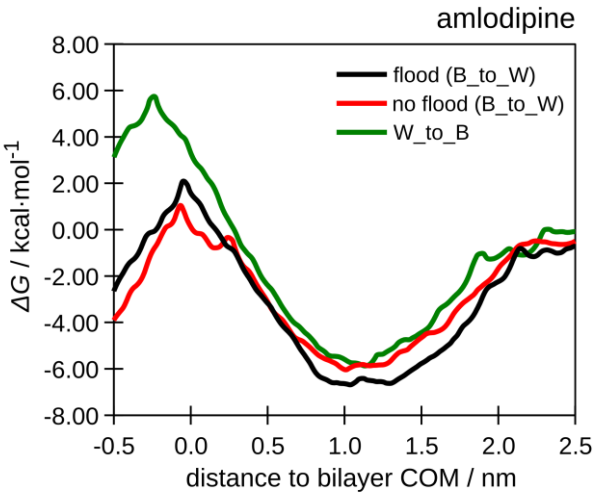

Figure S3. PMF considering three protocols for the AML compound. The black curve represents the umbrella sampling protocol comprising an additional flooding potential simulation, for each umbrella sampling window (*flood* protocol). The red curve depicts the same PMF without the application of the flooding potential (*no flood* protocol); and in green, we have the W_to_B umbrella sampling protocol. We extend the graphics until -0.3 nm, in order to check the symmetry of the profile at 0.0 nm (the bilayer center).

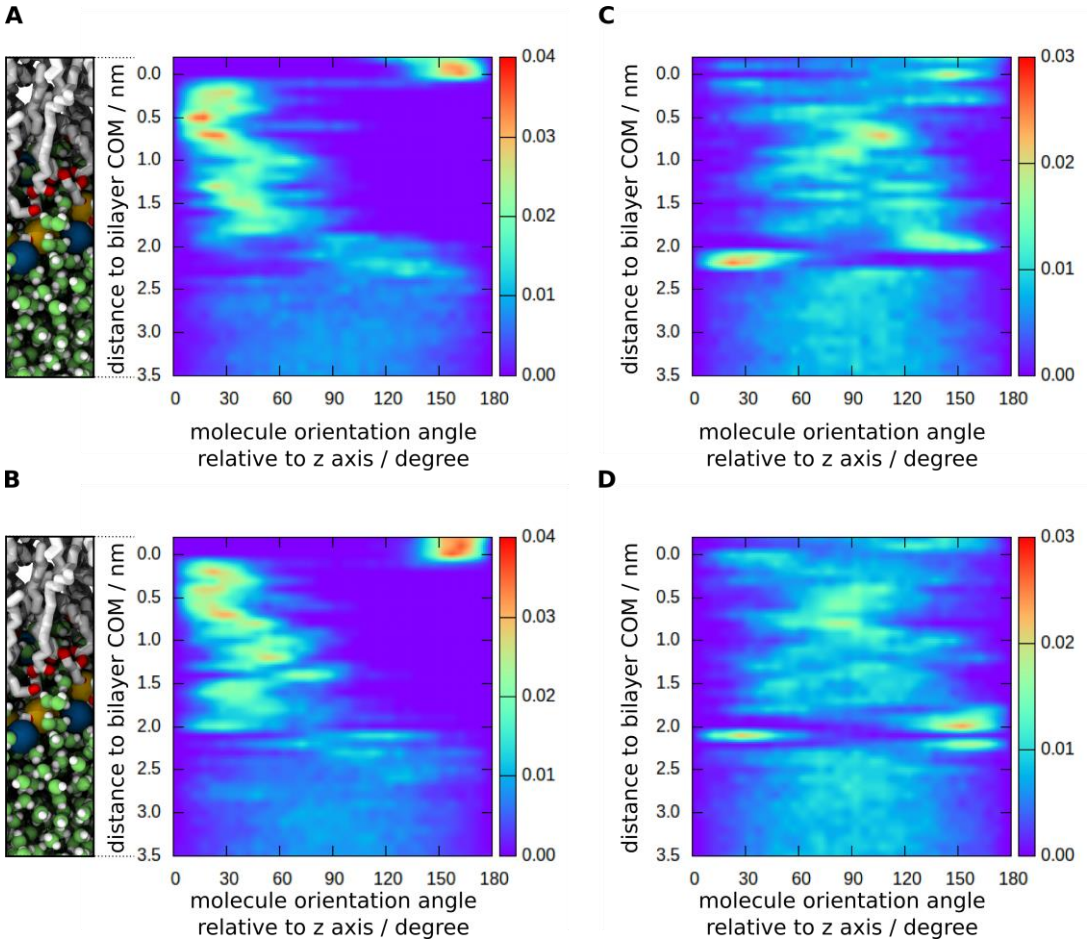

Figure S4. 5PA (A and B) and DBS (C and D) orientations relative to the bilayer normal axis (z axis). **A** and **C**. Umbrella sampling simulation for 5PA and DBS for the *no flood* protocol; **B** and **D**. Umbrella sampling simulation considering the *flood* protocol. On the left of plots A and B, we present a graphical representation of the bilayer's z axis projection (from -0.2 to 3.5 nm of the bilayers' center-of-mass distance).

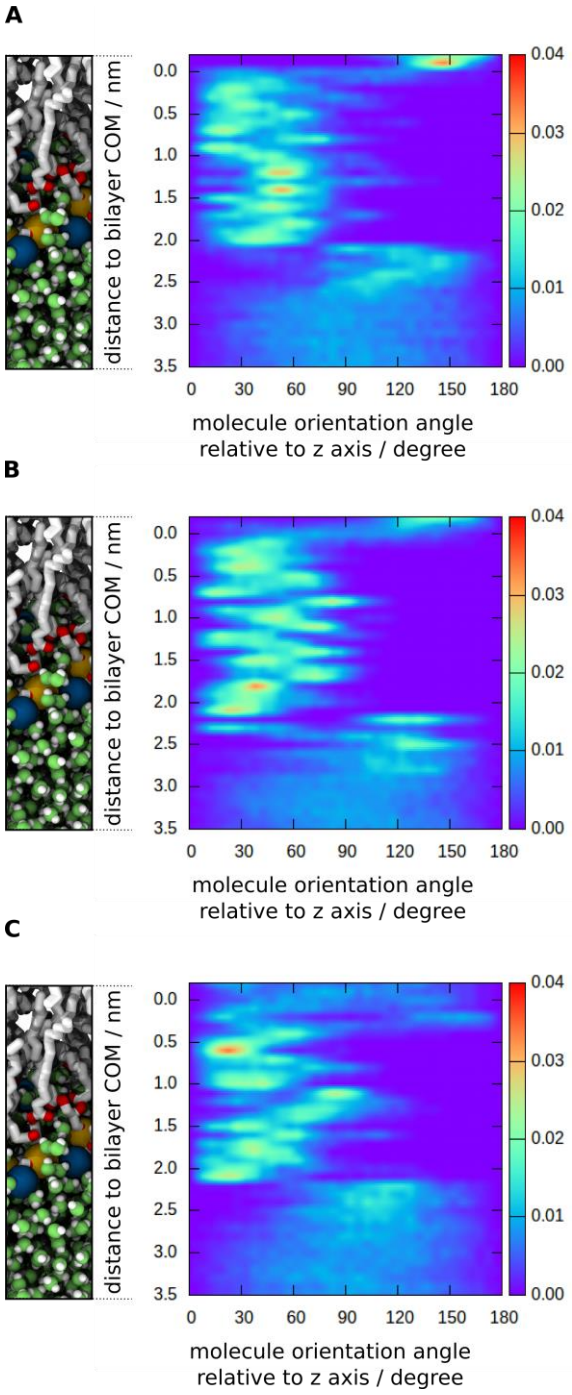

Figure S5. IBF orientation relative to the bilayer normal axis (z axis). **A.** *no flood* protocol; **B.** *flood* protocol employing a *cis* RESP charge distribution; and **C.** *flood* protocol employing a *trans* RESP charge distribution. On the left of each plot, we present a graphical representation of the bilayer's z axis projection (from -0.2 to 3.5 nm of the bilayers' center-of-mass distance).

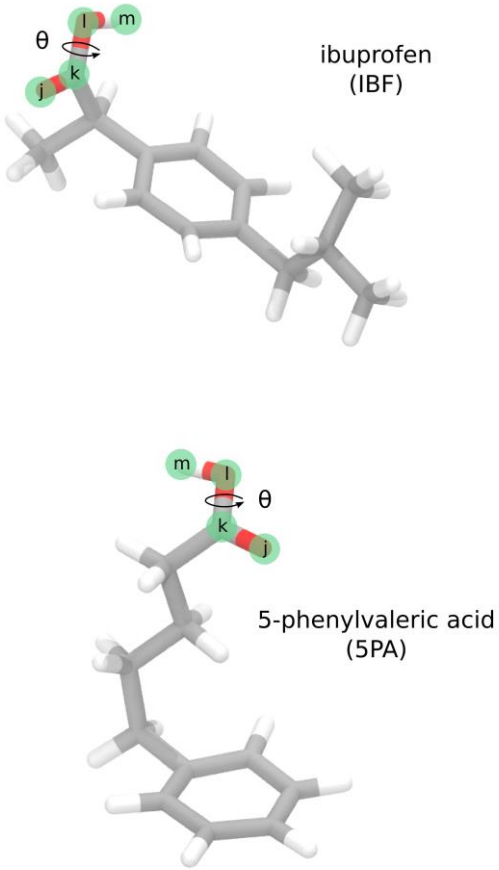

Figure S6. Graphical representation of the dihedral angle (θ) scanned during umbrella sampling simulations of 5PA and IBF inserted in TIP3P water boxes. This dihedral is also related to the two conformations (*cis* and *trans*) discussed in the main text.

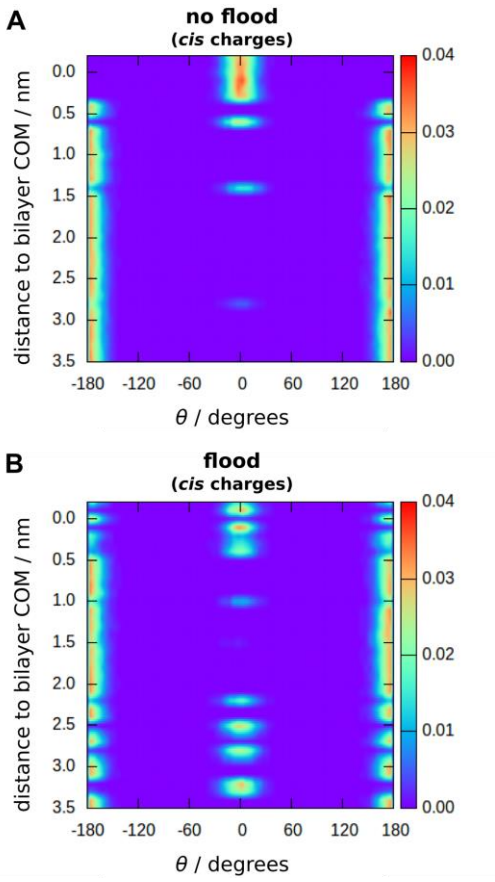

Figure S7. 5PA carboxylic acid dihedral distribution considering two umbrella sampling simulations. **A.** comprising the *no flood* protocol; **B.** considering the *flood* protocol.

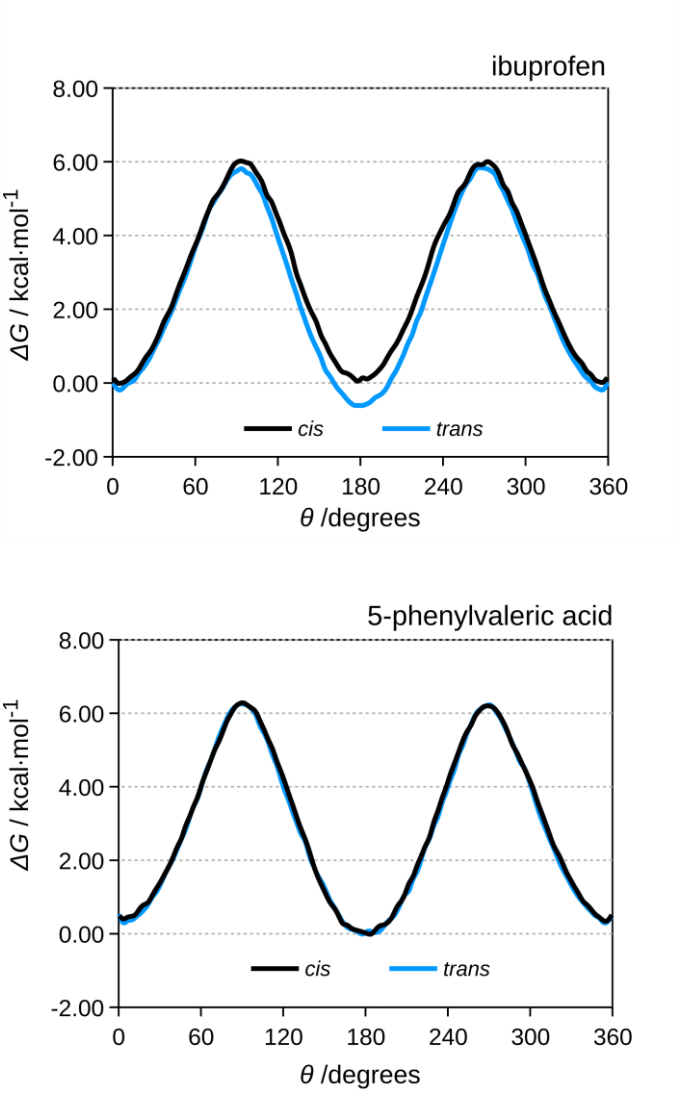

Figure S8. PMFs relative to the dihedral rotation comprising the COOH atoms of the carboxylic groups of 5PA and IBF. Both *cis* and *trans* RESP charges were considered, and are depicted for both molecules.

Section 3: PMFs' convergence

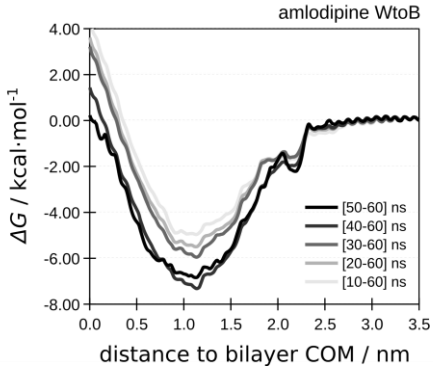

Figure S9. PMF convergence analyzed though superposition of the PMFs considering increasing umbrella sampling data (starting from the last structure). PMFs for the AML's W_to_B protocol is presented.

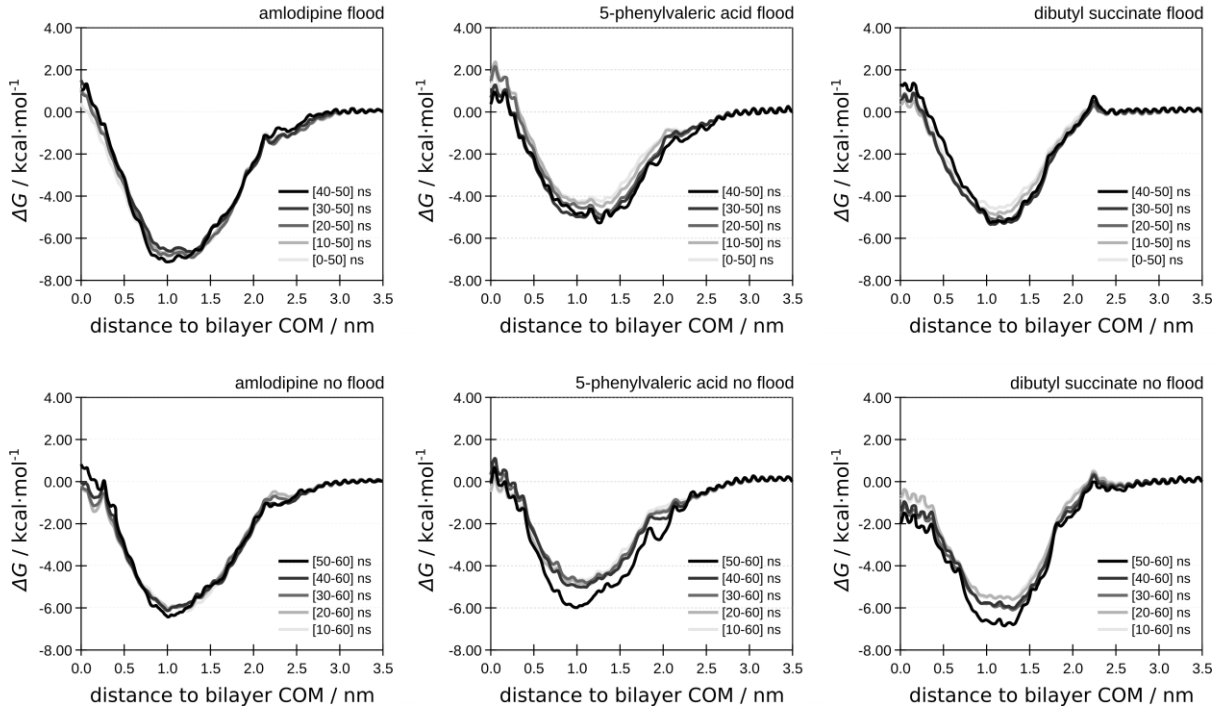

Figure S10. PMF convergence analyzed though superposition of the PMFs considering increasing umbrella sampling data (starting from the last structure). 5PA, AML, and DBS compounds are presented.

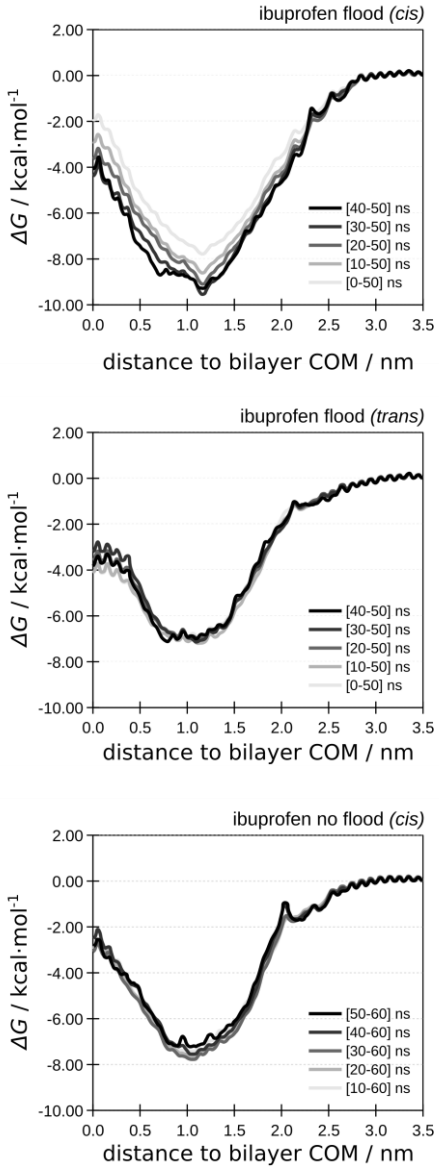

Figure S11. PMF convergence analyzed though superposition of the PMFs considering increasing umbrella sampling data (starting from the last structure) and considering IBF's different protocols.

REFERENCES

(1) Kucerka, N.; Nieh, M. P.; Katsaras, J., Fluid phase lipid areas and bilayer thicknesses of commonly used phosphatidylcholines as a function of temperature. *Bba-Biomembranes* **2011,** *1808* (11), 2761-2771.

(2) Kucerka, N.; Liu, Y. F.; Chu, N. J.; Petrache, H. I.; Tristram-Nagle, S.; Nagle, J. F., Structure of fully hydrated fluid phase DMPC and DLPC lipid bilayers using X-ray scattering from oriented multilamellar arrays and from large unilamellar vesicles. *Biophys. J.* **2005,** *88* (1), 245a-245a.

(3) Petrache, H. I.; Tristram-Nagle, S.; Nagle, J. F., Fluid phase structure of EPC and DMPC bilayers. *Chem. Phys. Lipids* **1998,** *95* (1), 83-94.

(4) Almeida, P. F. F.; Vaz, W. L. C.; Thompson, T. E., Lateral Diffusion in the Liquid-Phases of Dimyristoylphosphatidylcholine Cholesterol Lipid Bilayers - a Free-Volume Analysis. *Biochemistry-Us* **1992,** *31* (29), 6739-6747.

(5) Oradd, G.; Lindblom, G.; Westerman, P. W., Lateral diffusion of cholesterol and dimyristoylphosphatidylcholine in a lipid bilayer measured by pulsed field gradient NMR spectroscopy. *Biophys. J.* **2002,** *83* (5), 2702-2704.

(6) Filippov, A.; Oradd, G.; Lindblom, G., Influence of cholesterol and water content on phospholipid lateral diffusion in bilayers. *Langmuir* **2003,** *19* (16), 6397-6400.

(7) Douliez, J. P.; Leonard, A.; Dufourc, E. J., Restatement of Order Parameters in Biomembranes - Calculation of C-C Bond Order Parameters from C-D Quadrupolar Splittings. *Biophys. J.* **1995,** *68* (5), 1727-1739.

(8) Hess, B.; Bekker, H.; Berendsen, H. J. C.; Fraaije, J. G. E. M., LINCS: A linear constraint solver for molecular simulations. *J. Comput. Chem.* **1997,** *18* (12), 1463-1472.

(9) Bussi, G.; Donadio, D.; Parrinello, M., Canonical sampling through velocity rescaling. *J. Chem. Phys.* **2007,** *126* (1).

(10) Parrinello, M.; Rahman, A., Polymorphic transitions in single crystals: A new molecular dynamics method. *J. Appl. Phys.* **1981,** *52* (12), 7182-7190.

(11) Nosé, S.; Klein, M. L., Constant pressure molecular dynamics for molecular systems. *Mol. Phys.* **1983,** *50* (5), 1055-1076.

(12) Essmann, U.; Perera, L.; Berkowitz, M. L.; Darden, T.; Lee, H.; Pedersen, L. G., A Smooth Particle Mesh Ewald Method. *J. Chem. Phys.* **1995,** *103* (19), 8577-8593.

(13) Kumar, S.; Rosenberg, J. M.; Bouzida, D.; Swendsen, R. H.; Kollman, P. A., Multidimensional Free-Energy Calculations Using the Weighted Histogram Analysis Method. *J. Comput. Chem.* **1995,** *16* (11), 1339-1350.

(14) Hub, J. S.; de Groot, B. L.; van der Spoel, D., g_wham-A Free Weighted Histogram Analysis Implementation Including Robust Error and Autocorrelation Estimates. *J. Chem. Theory Comput.* **2010,** *6* (12), 3713-3720.

(15) Pastor, R. W.; Brooks, B. R.; Szabo, A., An Analysis of the Accuracy of Langevin and Molecular-Dynamics Algorithms. *Mol. Phys.* **1988,** *65* (6), 1409-1419.

(16) Berendsen, H. J. C.; Postma, J. P. M.; Vangunsteren, W. F.; Dinola, A.; Haak, J. R., Molecular-Dynamics with Coupling to an External Bath. *J. Chem. Phys.* **1984,** *81* (8), 3684-3690.

(17) Grossfield, A. *WHAM: the weighted histogram analysis method*.

(18) Humphrey, W.; Dalke, A.; Schulten, K., VMD: Visual molecular dynamics. *J. Mol. Graph. Model.* **1996,** *14* (1), 33-38.